Journal of ELECTRONIC MATERIALS, Vol. 49, No. 5, 2020
https://doi.org/10.1007/s11664-019-07680-y

TOPICAL COLLECTION: INTERNATIONAL CONFERENCE ON THERMOELECTRICS 2019

Parameter Matching and Optimization of an ISG Mild Hybrid Powertrain Based on an Automobile Exhaust Thermoelectric Generator

RUI QUAN ,[1,2,4] CHENGJI WANG,[2] FAN WU,[2] YUFANG CHANG,[1] and YADONG DENG[3]

1.—Hubei Key Laboratory for High-efficiency Utilization of Solar Energy and Operation Control of Energy Storage System, Hubei University of Technology, Wuhan, China. 2.—Agricultural Mechanical Engineering Research and Design Institute, Hubei University of Technology, Wuhan, China. 3.—School of Automobile Engineering, Wuhan University of Technology, Wuhan, China. 4.—e-mail: quan_rui@126.com

To improve the system efficiency and fuel economy of a traditional sport utility vehicle called "Warrior", a type of mild hybrid powertrain system based on the automobile exhaust thermoelectric generator (AETEG) and the integrated starter/generator (ISG) was established, and its parameter matching was optimized in this paper. Firstly, the effects of different components parameters on the performance index of the mild hybrid powertrain system were evaluated to decide the initial matching parameters. Then, all the component parameters of the ISG mild hybrid powertrain were optimized based on the designed control strategy and several different typical driving cycles. Finally, the AETEG model was established and embedded into the ADVISOR model of the ISG mild hybrid powertrain system, and both the dynamic property and fuel economy were analyzed. Simulation results under the Economic Commission for Europe plus extra-urban driving cycle (CYC_ECE_EUDC_LOW), Urban Dynamometer Driving Schedule, and the modified highway fuel economy test driving cycle demonstrate that, compared with the prototype vehicle, the dynamic property of the ISG mild hybrid powertrain system based on the AETEG is improved markedly, the fuel consumption is reduced by about 25%, and the battery charge is maintained between 75% and 51%. Road test experimental results also indicate that the maximum output power of the optimized AETEG is about 610 W, the maximum backpressure is below 1.8 kPa when the highest vehicle speed is 125 km/h. Parameter matching and optimization shows the promising potential of this type of AETEG for use in the ISG mild hybrid powertrain system.

Key words: Mild hybrid powertrain, automobile exhaust thermoelectric generator, integrated starter/generator, parameter matching, optimization

INTRODUCTION

Continuously updated development of green energy techniques is a good alternative to resolve the global energy crisis and increase environmental protection. Thermoelectric modules (TEMs) have several advantages such as little vibration, high

(Received July 3, 2019; accepted September 24, 2019; published online October 10, 2019)

reliability and durability, and no moving parts, so there has been considerable emphasis on their development for a variety of photovoltaic, automotive, military, aerospace, micro-generation and microelectronic applications over the years.[1–5]

With the rapid development of economy and society, automobiles have become a necessity all over the world. For the internal combustion engine used in traditional automobiles, only about 25% of fuel energy is converted to mechanical energy, whereas approximately 40% of fuel energy is wasted through exhaust gas, 30% is dissipated in the engine coolant, apart from friction and parasitic losses.[6] Thus, recovery of exhaust heat energy via thermoelectric technology for use in vehicle systems is a promising research subject, as it can enhance the overall output performance markedly. To achieve this goal, application of thermoelectric generators (TEGs) based on single, low, and intermediate temperature TEMs has been a novel research focus.[7,8]

It is well known that the hybrid powertrain system can improve overall efficiency compared with the traditional vehicle.[9] Recent research has validated that fuel consumption of the hybrid powertrain system can be further decreased and the environmentally harmful emissions markedly reduced by applying the generated power of TEGs.[10–15]

Because of the limited maximum output power (usually below 2000 W) and low overall efficiency (usually below 5%) of an automobile exhaust thermoelectric generator (AETEG) based on Bi_2Te_3 TEMs, it is suitable for the integrated starter/generator (ISG) mild hybrid powertrain system application after the optimization of TEM number and distribution pattern.[15] The ISG mild hybrid powertrain system based on the AETEG is also a complicated nonlinear system; for the convenience of analyzing its dynamic property, fuel economy and emission behavior, it is essential to first match the parameters of all the components to optimize the mild hybrid powertrain system.

ISG MILD HYBRID POWERTRAIN SYSTEM BASED ON AN AETEG

The existing mild hybrid powertrain system mainly includes a start–stop system, a belt-driven starter/generator (BSG) system and an ISG system.[16,17] Because the start–stop system can only accelerate the starting speed of engine, the BSG can't provide auxiliary power for vehicles. In this paper, the ISG system is considered in the mild hybrid powertrain system application.

The schematic diagram of the designed ISG mild hybrid powertrain system based on AETEG is shown in Fig. 1, it is mainly composed of an engine, an ISG, a direct current (DC)/DC converter, a battery group, a DC/alternating current (AC) inverter and an AETEG. The output of the AETEG is connected to a direct DC/DC converter, and its maximum power point is tracked by a DC/DC converter controller (DSP28335) to charge a battery group or power the ISG with a DC/AC inverter. All the controllers are connected by a controller area network (CAN) bus, and the energy management and control strategy is implemented by a vehicle controller.

VEHICLE PARAMETERS AND DESIGNED PERFORMANCE INDEX

Considering the available large space of chassis for the AETEG, as shown in Fig. 2, a prototype sport utility vehicle (SUV) called "Warrior" is adopted for the hybrid powertrain system; its basic parameters are listed in Table I, and the expected overall performances of the developed ISG mild hybrid powertrain system based on AETEG are listed in Table II.

PARAMETER DESIGN FOR THE ISG MILD HYBRID POWERTRAIN

As shown in Fig. 1, the designed ISG mild hybrid powertrain system based on AETEG is obviously a power-assisted structure, and its maximum power should be decided according to the power requirements with uniform speed provided as follows[18,19]:

$$P_1 = \frac{1}{3600\eta_t}\left(mgf + \frac{C_d A V^2}{21.15}\right)V \tag{1}$$

where P_1 is the minimum engine power, m is the SUV mass, g is the gravitational acceleration, η_t is the transmission efficiency, V is the SUV speed, f is the rolling resistance coefficient, C_d is the air resistance coefficient, and A is the face area.

The value of V should be decided based on the dynamic performance, according to the typical Chinese urban driving cycles,[20] as described in Eq. 2.

$$V_{aver} \le V \le V_{max} \tag{2}$$

where V_{aver} is the average speed (20–30 km/h), V_{max} is the maximum speed (80 km/h) in the urban driving cycle.

Meanwhile, according to Table II, when the ISG mild hybrid powertrain system is driven by only engine, it can maintain at 40 km/h with a 10% grade. Thus, the demanded engine power (denoted P_2) is calculated by Eq. 3 based on the kinetic theory of vehicle.[18,19]

$$P_2 = \frac{1}{3600\eta_t}\left(mgf\cos\theta + mg\sin\theta + \frac{C_d A V^2}{21.15}\right)V \tag{3}$$

Moreover, to accelerate the ISG mild hybrid powertrain system from 0 to 120 km/h within 20 s with only engine, on this occasion, the demanded engine power (denoted P_3) is calculated in Eq. 4.

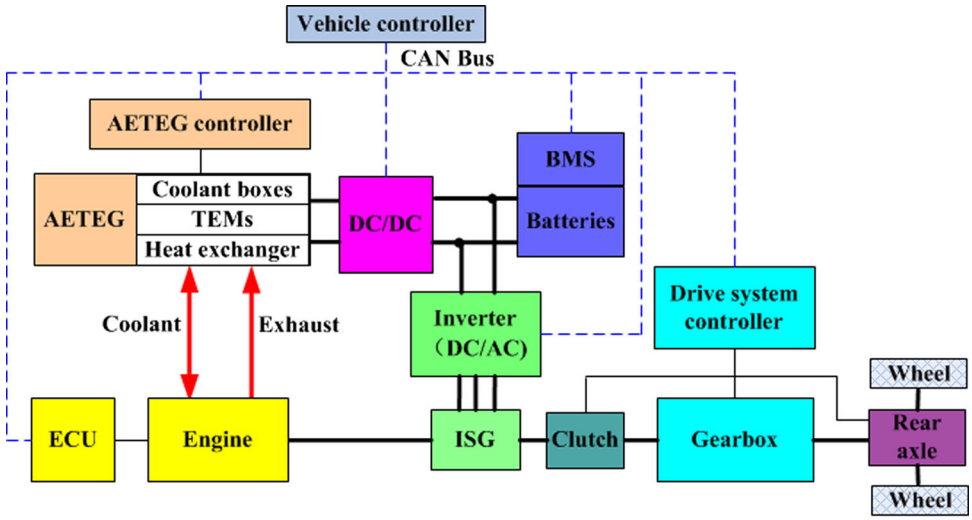

Fig. 1. Schematic of the ISG mild hybrid powertrain system based on an AETEG.

Fig. 2. Prototype SUV called "Warrior".

$$P_3 = \frac{1}{3600\eta_t}\left(mgf + \frac{C_d A V^2}{21.15} + \delta\frac{dV}{dt}\right)V \qquad (4)$$

where δ is the rotational mass conversion coefficient (1.01), $\frac{dV}{dt}$ is the late acceleration (0.556).

Combining the requirements from Eqs. 1 to 4, the calculated minimum engine power is 45 kW, and the maximum engine power is 122 kW. Considering the consumed power (about 8 kW) for auxiliary devices such as air conditioner, wiper and lights, and the power margin (above 10%) to charge the batteries, the original required engine power is set to be about 100 kW.

When the rotating speed of the ISG is below its rated value, its torque value is constant. While the rotating speed is above the rated value, its output power is constant. The corresponding parameters of the ISG are the rated power (denoted P_r), the maximum power (denoted P_{max}), the rated rotating speed (denoted N_r) and the maximum rotating speed (denoted N_{max}).

Considering the engine rotating speed usually changes from 1200 rpm to 3800 rpm, the gearbox ratio is 2, and the rated rotating speed of ISG should be between 2400 rpm and 7600 rpm, it is set at 5000 rpm. For the increased constant power coefficient (denoted β) is from 2 to 4, in this paper, β is set

Table I. Basic parameters of the prototype SUV

Parameter	Value
Kerb weight	3250 kg
Load weight	1750 kg
Coefficient of air resistance	0.61
Coefficient of rolling resistance	0.013
Face area	5.17 m^2
Dimensions	4694 mm*2134 mm*2430 mm
Minimum ground clearance	410 mm
Maximum power	112 kW (2700 rpm)
Maximum torque	502 nm (1500 rpm)
Engine capacity	3900 cc
Gearbox	4AT
Wheel base	3300 mm
Front gauge	1820 mm
Track rear	1820 mm
Tyre type	37 × 12.5 R16.5
Drive mode	4-wheel steering
Transmission efficiency	0.85

Table II. Expected performances of the ISG mild hybrid powertrain system based on AETEG

Parameter	Value
Acceleration time from 0 km/h to 80 km/h	< 15 s
Gradeability	40%
Climbing speed with 10% grade	40 km/h
Fuel economy (urban driving cycle)	Decreasing by 20% (original value: 13.6L/100 km)
Maximum speed	> 120 km/h

as 2, thus, the designed maximum rotating speed of the ISG is 10000 rpm.

Furthermore, the ISG usually drives vehicle without engine or accelerate vehicle, it should start the engine in a quite short time, and its accelerated speed can be described as follows:

$$\frac{dV}{dt} = \frac{F_t - F_w - F_f}{\delta_{ISG} m} \tag{5}$$

where F_t is the driving force, F_w is the air resistance, F_f is the rolling resistance, and δ_{ISG} is the rotational mass conversion coefficient. As shown in Fig. 1, δ_{ISG} can be calculated by Eq. 6.

$$\delta_{ISG} = 1 + \frac{I_w + (I_e + I_m) i_g^2 i_0^2}{m r^2} \tag{6}$$

where I_w is the rotational inertia of wheels, I_e is the rotational inertia of engine's output shaft, I_m is the rotational inertia of ISG output shaft, i_g is the gearbox ratio, and i_0 is the rotational inertia of rear axle.

Moreover, the acceleration time (denoted T) from 0 to V is described as follows:

$$T = \frac{1}{3.6} \int_0^v \frac{dt}{dv} \cdot dv = \frac{1}{3.6} \int_0^v \frac{\delta \cdot m}{F_t - F_w - F_f} \cdot dv \tag{7}$$

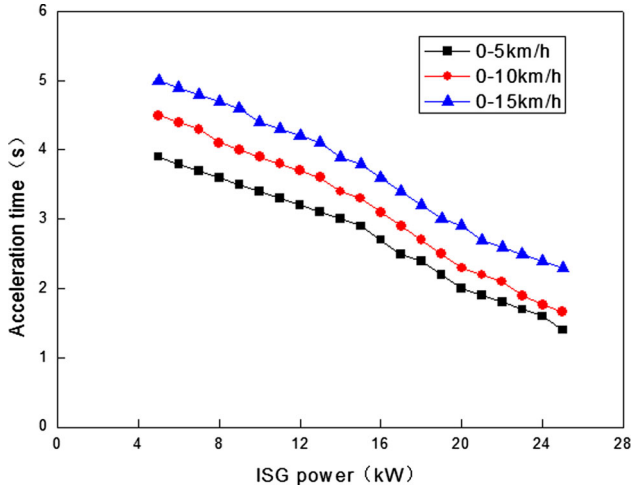

Fig. 3. Acceleration time between different ISG power and vehicle speeds.

Based on the Economic Commission for Europe (ECE) plus extra-urban driving cycle (EUDC), i.e. CYC_ECE_EUDC_LOW, the simulated results of acceleration time between different ISG power and vehicle speeds by combining the above parameters into ADVISOR 2002 are shown in Fig. 3. When the

vehicle speed is 20 km/h during the pure electric mode, according to Eq. 1, the calculated minimum ISG power should be above 10 kW. For the acceleration time of prototype SUV from 0 km/h to 5 km/h, 0 km/h to 10 km/h, 0 km/h to 15 km/h is 2.1 s, 2.8 s and 3.4 s, respectively, to ensure the dynamic performance of ISG mild hybrid powertrain system based on AETEG is above the prototype SUV, and considering the regenerative braking ability, the final maximum ISG power should be above 20 kW; the corresponding acceleration time of prototype SUV from 0 km/h to 5 km/h, 0 km/h to 10 km/h, 0 km/h to 15 km/h is 2 s, 2.4 s and 2.9 s, respectively.

Usually, the voltage level of the alternating current motor is 288 V, 336 V, and 600 V and so on. In this paper, the lithium iron phosphate ($LiFePO_4$) batteries are applied as a battery group in the ISG mild hybrid powertrain, and the corresponding rated voltage is 288 V; because the rated voltage of each single battery is 3.2 V, there are 90 single batteries connected in series.

When the ISG power is 20 kW, supposing the efficiency of the ISG (denoted η_{ISG}) is 90% and that of the DC/AC inverter (denoted η_{inv}) is 93%, the required minimum power of the battery group (denoted P_{Bat}) is calculated according to Eq. 8.

$$P_{Bat}=\frac{P_{max}}{\eta_{ISG}\cdot\eta_{inv}}=23.9\,kW \tag{8}$$

Because TEMs based on Bi_2Te_3 are the most common and commercially available until now, the designed AETEG shown in Fig. 1 is developed with the Bi_2Te_3 based TEMs. According to our previous experimental results,[21] the maximum power of a single TEM is approximately 6 W when its maximum temperature difference is 250°C, and its average power is about 4.5 W when the temperature difference is 200°C. Because the coolant temperature of the engine is roughly 90°C, the maximum operating temperature of the TEM is 350°C, and considering the heat loss and power generation efficiency, the average power of a singe TEM is 4 W. To make full use of the prototype SUV chassis space, the AETEG with four TEGs connected in parallel with an exhaust pipe was developed.

Each specific TEG, as illustrated in Fig. 4, consists of several TEMs, a brass heat exchanger, several cooling units and so on. All the TEMs are sandwiched between the two surfaces of the heat exchanger connected to an engine exhaust pipe and cooling units consisting of six pairs of water tanks, called single-row cooling boxes, and they are clamped with adjustable force using four concave-type steel and torque wrenches. In total, there are 60 TEMs of Bi_2Te_3 based materials arranged on both surfaces of a brass heat exchanger in six rows, i.e. five TEMs in each row are placed under a corresponding aluminum alloy cooling box, all the cooling boxes and the TEMs of each TEG are connected in series.[22]

Furthermore, to obtain a relatively uniform temperature distribution and efficient heat transfer performance, the implemented each heat exchanger is a chaos-shaped internal structure,[22,23] its effective heat transfer size is 400 mm in length and 300 mm in width. For each cooling unit above one surface of a heat exchanger, six single-row cooling boxes are connected in series for the sake of convenient assembly. For the maximum operating temperature of conventional Bi_2Te_3 TEM is 200°C–250°C, the adopted Bi_2Te_3 TEMs in this study are manufactured by Thermonamic Electronics (Jiangxi, China) Corp. Ltd, the specific dimensions are 56 mm × 56 mm × 6 mm, and the high conductivity graphite paper whose maximum operating temperature is 350°C is used as the thermal conductive interface material of Bi_2Te_3 TEMs.[23]

Considering the large available space of the prototype SUV, an AETEG system with four of the above TEGs thermally connecting in parallel (i.e., all inlets of four heat exchangers and cooling systems of each TEG are connected in parallel) and electrically connecting in series is constructed, which includes 240 single TEMs in total, whose

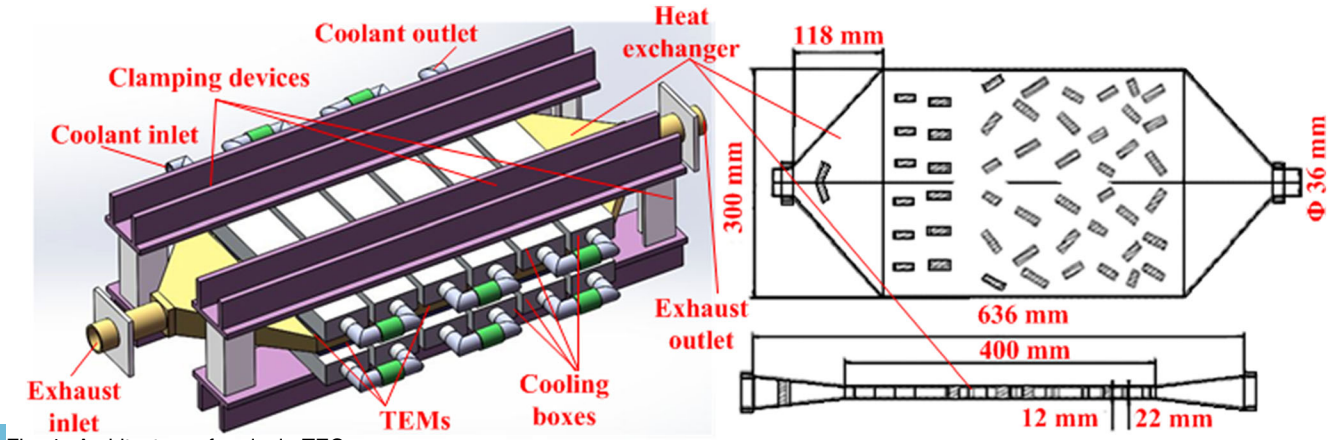

Fig. 4. Architecture of a single TEG.

dimensions are 1420 mm × 670 mm × 185 mm, and a terrain clearance of 315 mm. For the cooling unit, a branch circle of engine coolant is adopted without a pump or radiator for the sake of saving installation space and reducing extra consumed power.

The most important parameter of both gearbox and rear axle is the gear ratio, and the maximum gear ratio is decided by the maximum vehicle gradeability, while the minimum gear ratio depends on the maximum vehicle speed.

As shown in Table II, the expected maximum gradeability is 40%, and the expected maximum vehicle speed is 100 km/h; both the calculated maximum and minimum gear ratios based on the gear ratio distributions with different gearbox gears are given in Table III.

PARAMETERS OPTIMIZATION

According to the initial parameters matching of each component of the above ISG hybrid powertrain system, they are optimized based on the designed control strategy and different driving cycles.

Because the energy control strategy directly affects the performance index of the hybrid powertrain system, and considering the above dynamic requirements, to optimize the efficiency of the engine, the ISG, the batteries, the AETEG and the SUV, a flow chart of the proposed control strategy is created and shown in Fig. 5. Firstly, the vehicle starts according to the vehicle speed and accelerator pedal signals. Then, the vehicle controller controls gear changes when the engine power meets the requirements. Finally, it preliminarily selects the working mode based on the optimal vehicle efficiency and the running status of the hybrid powertrain. Once the working mode is decided, the optimal torque distribution is figured out, and the maximum power point tracking (MPPT) of the AETEG is adopted by combining perturb and observe (P&O) algorithm, quadratic interpolation and constant voltage tracking method[24,25] to charge the batteries or supply relatively tiny power to the ISG.

Based on the above initial designed parameters, the DCEC engine (B series type) is adopted, and the selected parameter-matching matrix among the engine, the ISG, batteries and different driving cycles are provided in Table IV. In theory, there are 24 (i.e. 2 × 2 × 2 × 3) different types of combining schemes. Some simulated calculating matrix results based on several typical types of

Table III. The gear ratio parameters of gearbox and rear axle

First gear	Second gear	Third gear	Fourth gear	Rear axle
3.47	2.458	1.569	1.0	4.04

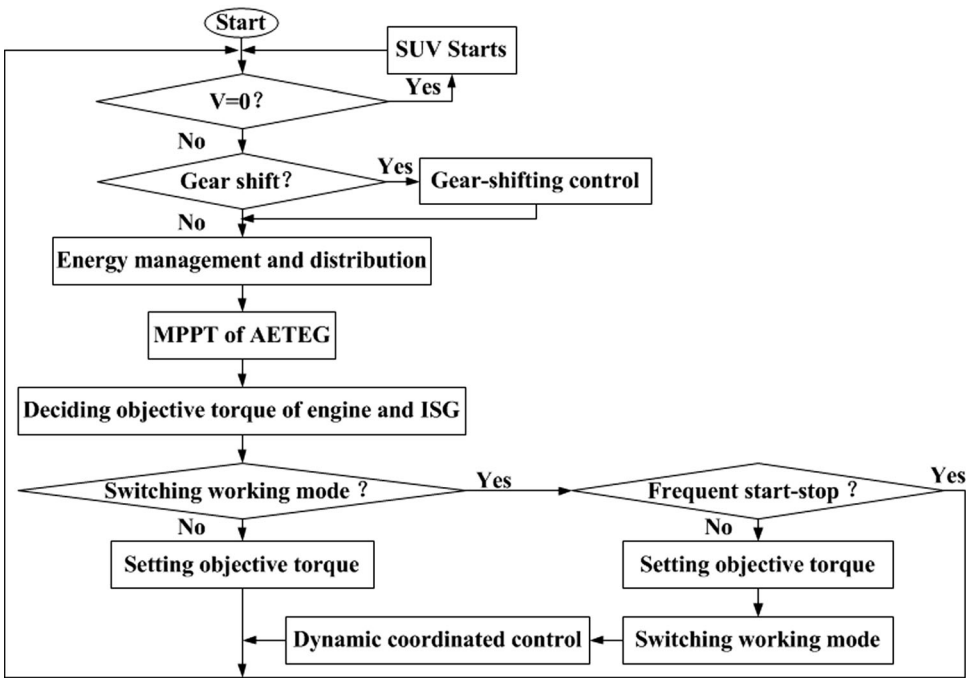

Fig. 5. Flow chart of the proposed control strategy.

Table IV. The component matching matrix

Engine (kW)	ISG (kW)	Batteries (kW)	Drive cycle
95	20	20	CYC_UDDS
105	25	30	CYC_ECE_EUDC_LOW
95	25	30	CYC_HWFET

Table V. The simulated component matrix

Engine (kW)	ISG (kW)	Batteries (kW)	Average fuel economy (L/100 km)	Fuel consumption decreased by (%)
95	20	20	11.4	17.2
105	20	20	11.8	14.1
95	25	20	10.9	19.9
105	25	20	11.7	15.3
95	20	30	10.8	21.2
105	20	30	11.5	16.3
95	25	30	10.6	22.6
105	25	30	11.6	15.8

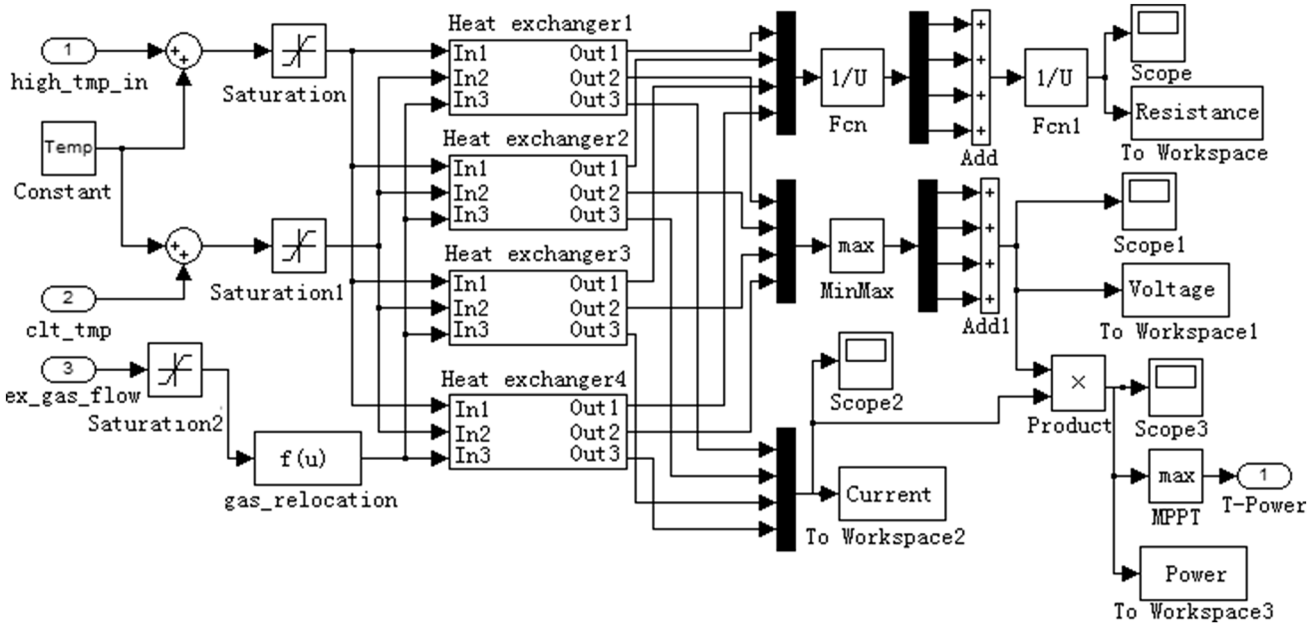

Fig. 6. Simulink model of AETEG including four heat exchangers.

combined schemes are presented in Table V, and it can be concluded that when the engine power is 95 kW, the ISG power is 20 kW and the batteries power is 30 kW, the fuel consumption of SUV can be decreased by at least 20%, which meets the develop requirements in Table II.

PERFORMANCE ANALYSIS

For the 240 TEMs of Bi_2Te_3 based materials used in AETEG, the AETEG model based on test data is expressed as follows[26,27]:

$$V_{\mathrm{AETEG}} = \sum_{i=1}^{240} n\alpha_{\mathrm{PNi}}\Delta T_i = n(\alpha_{pi} - \alpha_{ni})(T_{\mathrm{Hi}} - T_{\mathrm{Li}}) \quad (9)$$

$$R_{\mathrm{AETEG}} = \sum_{i=1}^{240} R_i = 240(nl_p/(\sigma_p A_p) + nl_n/(\sigma_n A_n)) \quad (10)$$

$$\alpha_{\mathrm{PNi}} = \left(22224 + 930.6 \times 0.5 \times \Delta T_i - 0.9905 \times (0.5 \times \Delta T_{\mathrm{i}})^2\right) \times 10^{-9} \tag{11}$$

where V_{AETEG} and R_{AETEG} are the open circuit voltage and internal resistance of AETEG, respectively. α_{PNi} is the relative Seebeck coefficient (V/K), α_{pi} and α_{ni} are the Seebeck coefficients of the p-type and the n-type semiconductor galvanic arms, respectively. T_{Hi} and T_{Li} are the hot side and cold side temperatures (K), respectively. l_p, σ_{p}, A_{p} are the leg length (m), electricity resistivity (Ωm) and cross-sectional area (m^2) of a p-type semiconductor galvanic arm, respectively, while l_n, σ_{n}, A_{n} are the leg length, electricity resistivity and cross-sectional area of an n-type semiconductor galvanic arm, respectively.

The output power of the AETEG reaches its maximum value (denoted *T_Power*) when the external load resistance is equal to its internal resistance, and is expressed as:

$$T\_Power = U_{\mathrm{AETEG}}^2/(4R_{\mathrm{m}}) \tag{12}$$

Based on the thermoelectric conversion and above nonequilibrium thermodynamics theory, the established Simulink model of the AETEG including four heat exchangers is shown in Fig. 6. It includes three input parameters, namely, the outlet exhaust gas temperature of the three-way catalyst (i.e. the inlet temperature of heat exchangers, denoted *high_tmp_in*), engine coolant temperature (i.e. the cold side temperatures of AETEG, denoted *fc_ctl_tmp*), and exhaust gas flow of the three-way catalyst (denoted *ex_gas_flow*). The output parameter is the maximum output power of the AETEG based on MPPT algorithm (stated in the next section). Thus, the maximum output power of the AETEG can be treated as a non-linear function of *high_tmp_in*, *ex_gas_flow* and *fc_ctl_tmp*, which are affected by both the vehicle speed and the engine torque.

There are many different types of commercially available lithium batteries implemented in new energy vehicles. For the above ISG mild hybrid power, lithium iron phosphate batteries in series are adopted. When the depth of discharge (DOD) is maintained between 30% and 70%, the charge and discharge curve of batteries can be treated as linear, and the equivalent circuit model is shown in Fig. 7.[28] Obviously, it is a second-order linear model recommended by the partnership for a new generation of vehicles (PNGV).

Once the parameters R_1, C_1, R_2, C_2, E are confirmed, the equivalent circuit model can be established. The steady voltage E can be directly tested, while the parameters R_1, C_1, R_2 and C_2 are difficult to experiment with, as they impose typical input signals because of their time-varying characteristics. Thus, they are evaluated online with

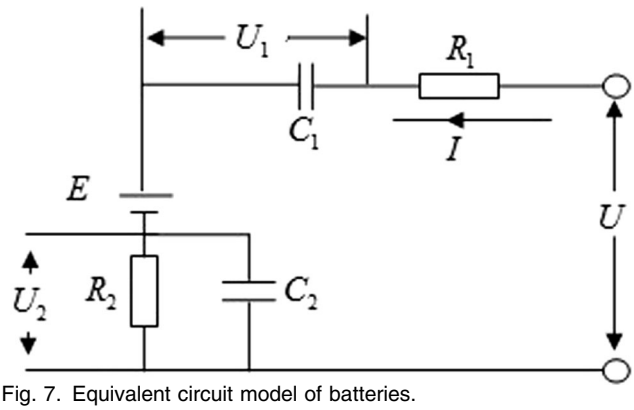

Fig. 7. Equivalent circuit model of batteries.

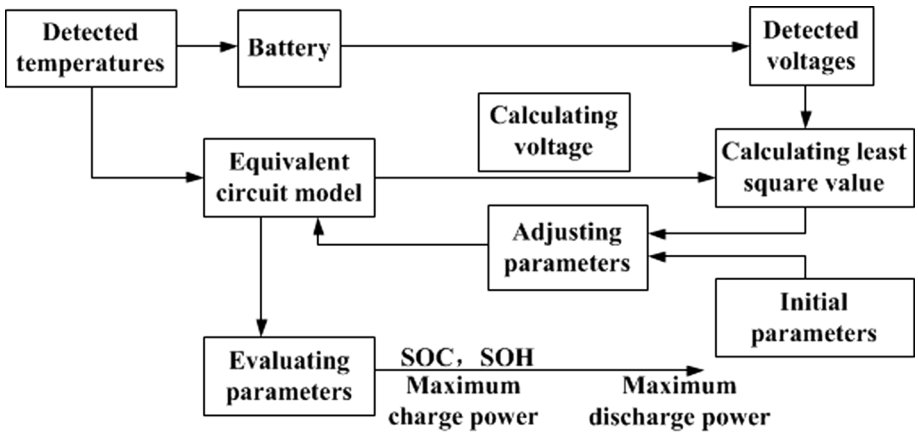

Fig. 8. Online identification model process of batteries.

excitation signal I and output response U, and the corresponding online identification model process is shown in Fig. 8.

According to the battery characteristics, the parameter C_1 can be treated as a constant since it is not markedly affected by the exterior environment and service life. When the batteries start to work, their open-circuit voltages are tested with a battery management system (BMS), the parameters R_1, R_2 and C_2 are identified with the least-square methods, and the state of health (SOH) is calculated. For the important state of charge (SOC) parameter, it is evaluated based on calculating the ampere hour, which is given as follows[29]:

$$\mathrm{SOC} = \begin{cases} \mathrm{SOC}_0 - \dfrac{\sum I_b \cdot \Delta t}{3600 \cdot C_b(I_b, T)} & I_b \geq 0 \\ \mathrm{SOC}_0 - \dfrac{\eta_b \cdot \sum I_b \cdot \Delta t}{3600 \cdot C_b(I_b, T)} & I_b < 0 \end{cases} \quad (13)$$

where Δt is the simulated step length (s), $C_b(I_b, T)$ is the real-time battery capacity (AH), SOC_0 is the initial SOC value (set at 75%), η_b is the charge efficiency, T is the battery temperature (°C).

To analyze the performance of the ISG mild hybrid powertrain system based on AETEG, the embedded module "PARALLEL_SA_defaults_in" of ADVISOR[30] is modified and added with the above simulation models of AETEG and batteries, the overall vehicle simulation model of ISG mild hybrid powertrain based on AETEG is shown in Fig. 9, the maximum output power is connected to the power bus module for the energy distribution, and the dynamic performance of the hybrid powertrain system is analyzed based on CYC_ECE_EUDC_LOW driving cycle.

The acceleration performance comparison is given in Fig. 10, the continuous climbing speed with a 10% grade of the ISG mild hybrid powertrain system is shown in Fig. 11, the overall comparison between the ISG mild hybrid powertrain and the prototype SUV based on CYC_ECE_EUDC_LOW is listed in Table VI. It demonstrates that the acceleration time (from 0 km/h to 120 km/h) and the maximum speed of the ISG mild hybrid powertrain based on AETEG are 18.9 s and 140 km/h, respectively, while the acceleration time (from 0 km/h to 120 km/h) and maximum speed of the prototype

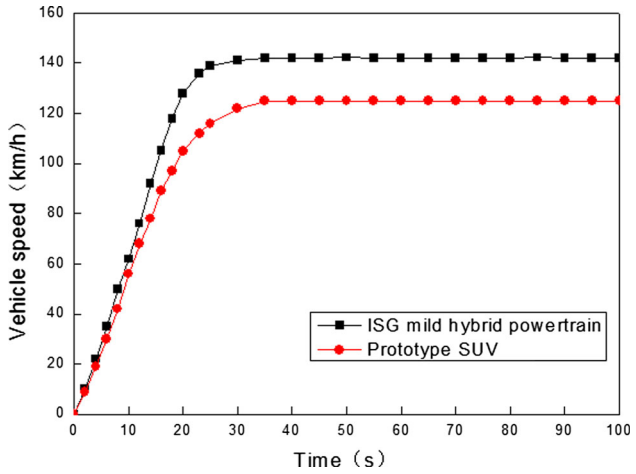

Fig. 10. Acceleration performance comparison between ISG mild hybrid powertrain and prototype SUV.

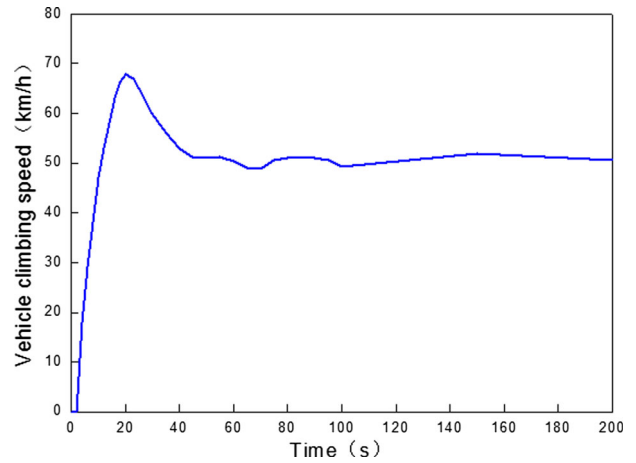

Fig. 11. Climbing speed with 10% grade of ISG mild hybrid powertrain system.

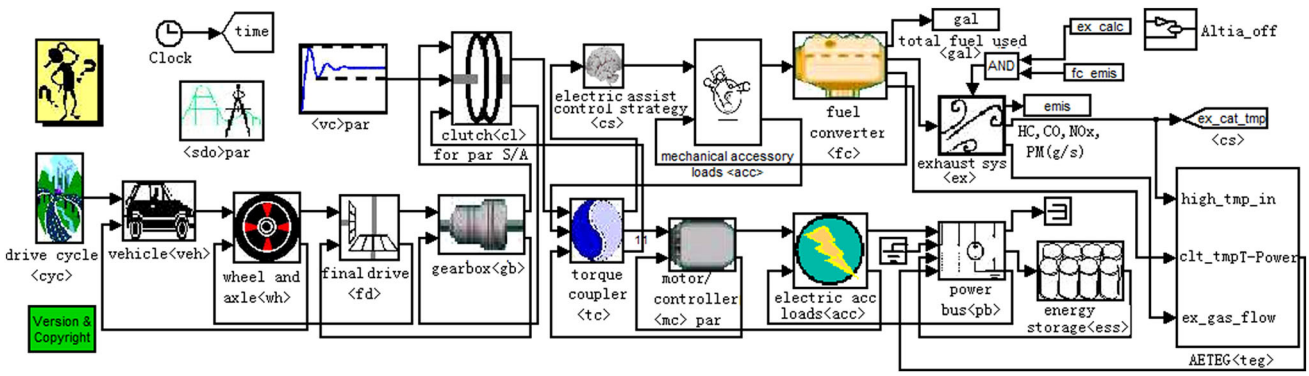

Fig. 9. Simulation model of ISG mild hybrid powertrain based on AETEG.

Table VI. Dynamic performance comparison between ISG mild hybrid powertrain and prototype SUV

Items	ISG mild hybrid powertrain	Prototype SUV
0–10 km/h	2.1 s	2.6 s
0–30 km/h	5.0 s	6.3 s
0–50 km/h	8.1 s	9.4 s
0–70 km/h	10.9 s	12.5 s
0–90 km/h	13.8 s	16.6 s
0–120 km/h	18.9 s	24.2
Maximum speed	142 km/h	125 km/h
Maximum gradeability	51.3%	40.6%
Climbing speed with 10% grade	51 km/h	39 km/h

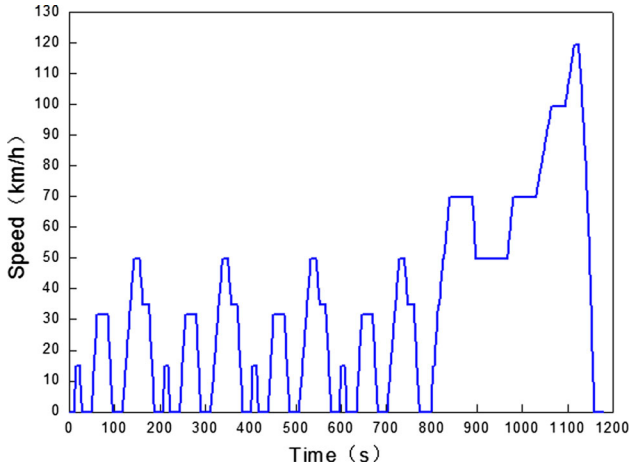

Fig. 12. CYC_ECE_EUDC_LOW driving cycle.

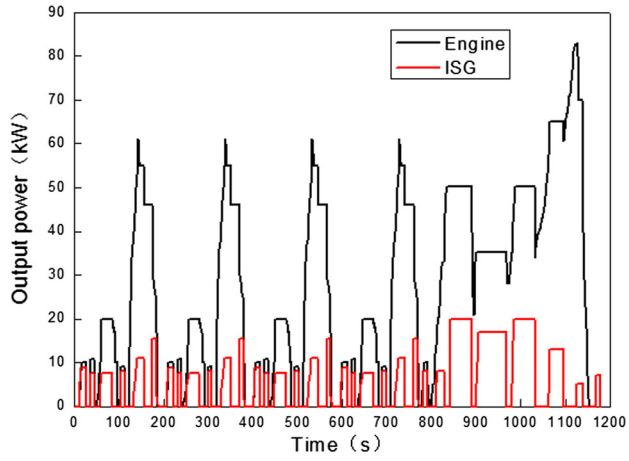

Fig. 13. Output power of both engine and ISG based on CYC_ECE_EUDC_LOW.

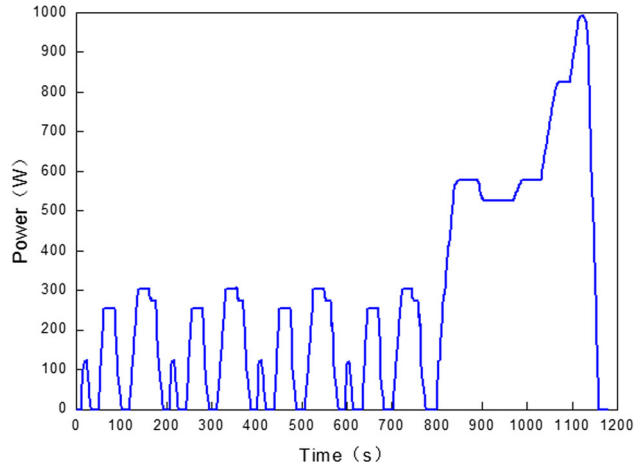

Fig. 14. Maximum output power of AETEG.

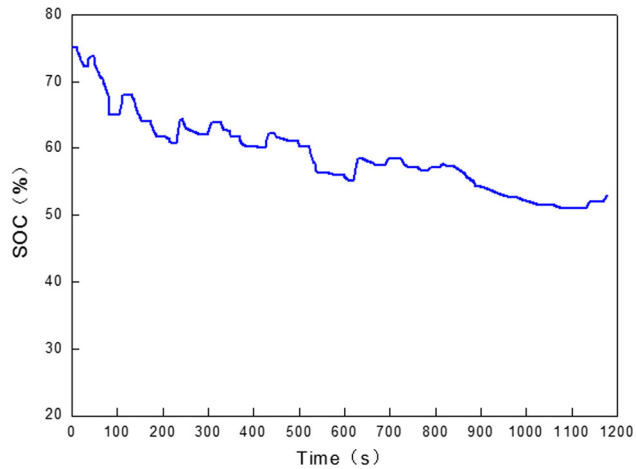

Fig. 15. SOC changing curve of batteries.

SUV are 24.2 s and 125 km/h, respectively. The dynamic performance of the designed ISG mild hybrid powertrain is superior to the prototype SUV with similar output power, and it meets the develop requirements presented in Table II.

According to the above final parameter matching results and the ADVISOR model of the ISG mild hybrid powertrain system, the output power of both the engine and the ISG based on CYC_ECE_EUDC_LOW driving cycle[30] given in Fig. 12 is shown in Fig. 13, the maximum output power of AETEG based on the hybrid MPPT algorithm[24] is provided in Fig. 14, and the corresponding SOC changing curve of batteries is provided in Fig. 15. This indicates that the engine works within its high-efficiency area with the above designed control strategy, the maximum output power of the AETEG is proportional to the vehicle speed, and the SOC of batteries remains relatively steady (between 75%

Table VII. Fuel economy performance comparison

Driving cycles	Average fuel economy(L/100 km)		Fuel economy improved by (%)
	ISG mild hybrid powertrain	Prototype SUV	
CYC_UDDS	11.3	15.7	28.1
CYC_EUDC_LOW	11.1	14.9	25.5
CYC_HWFET	10.4	13.8	24.6

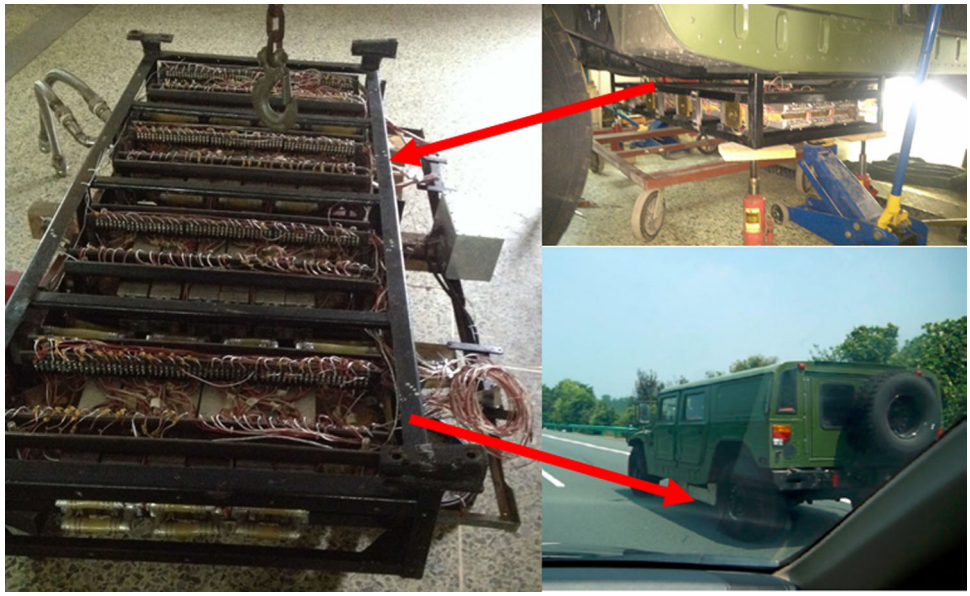

Fig. 16. Road test object map of AETEG used in prototype SUV.

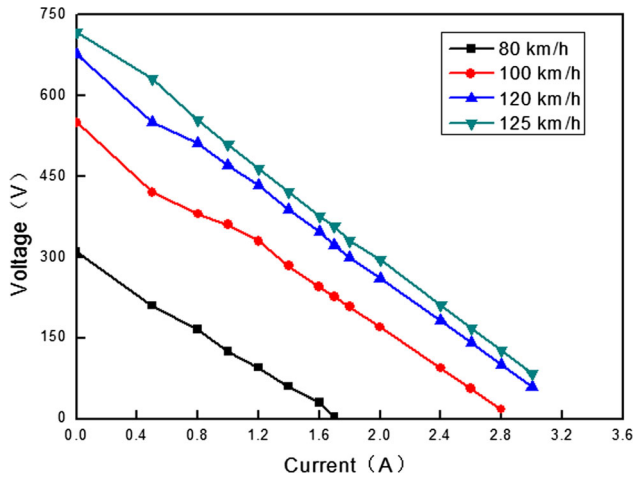

Fig. 17. Output voltage versus current curves of AETEG with several typical SUV speeds.

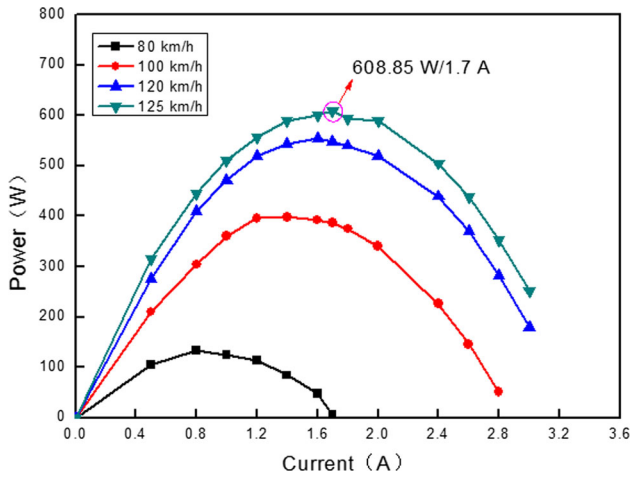

Fig. 18. Power versus current of AETEG with several typical SUV speeds.

and 51%) during the whole CYC_ECE_EUDC_LOW driving cycle.

The fuel economy performance in Table VII is also analyzed and compared based on different driving cycles. It can be concluded that the fuel economy is affected by different driving cycles. Compared with the prototype SUV with the same control strategy, the fuel consumption of the ISG mild hybrid powertrain system based on AETEG has been reduced by 28.1% (11.3 L/100 km), 25.5% (11.1 L/100 km), and 24.6% (10.4 L/100 km), respectively, when the corresponding driving cycles are CYC_UDDS, CYC_ECE_EUDC_LOW and CYC_HWFET, which also meets the design requirements listed in Table II.

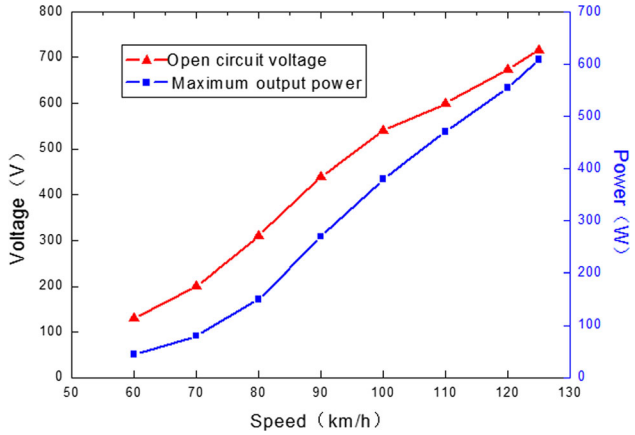

Fig. 19. Open circuit voltage and maximum output power of AETEG with different SUV speeds.

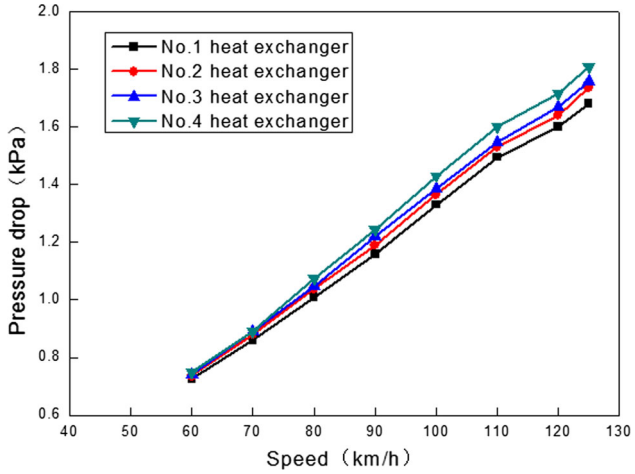

Fig. 20. Pressure drops of four chaos-shaped heat exchangers with different SUV speeds.

The road test object map of the AETEG used in the prototype SUV is shown in Fig. 16. The dimensions of the AETEG are 1420 mm × 670 mm × 185 mm, and its terrain clearance is 315 mm. For its cooling system, a branch circle of engine coolant is adopted without pump and radiator for the sake of saving installation space and reducing extra consumed power. The road test is carried out on the Wuhan–Huangshi expressway of China, the clamping pressure is 300 kg/m^2, and the engine coolant flow rate is 40.8 L/min, the measured characteristics curves of output voltage and power versus current with several typical SUV speeds is shown in Figs. 17 and 18, respectively. The open circuit voltage and maximum output power of the AETEG with different SUV speeds are described in Fig. 19. It is obvious that the output voltage and power of the designed AETEG are in direct proportion to the SUV speeds, increasing both output voltage and power with the same external load are accompanied with the augment of the SUV speeds. When the highest SUV speed is 125 km/h, the measured maximum output power of the AETEG is 608.9 W.

Undoubtedly, the backpressure will be increased due to the AETEG as an addition to the engine of prototype SUV, and the influence of the exhaust gas backpressure (i.e. pressure drop) on the engine plays a significant role in the prototype SUV fuel economy and emission performance. Therefore, minimizing the unwanted backpressure increase by optimizing heat exchangers of the AETEG is important. Pressure drop experiements are performed for the above four chaos-shaped heat exchangers and the results are shown in Fig. 20. It can be concluded that the backpressure is accompanied by the augmentation of the prototype SUV speeds, and the pressure drops from the inlet to outlet corresponding to the four chaos-shaped heat exchangers are similar at the same speed. The difference among them caused by the different branch structures of the manifold is within 10%. When the speed of the prototype SUV increases to 125 km/h, the maximum pressure drops of four heat exchangers are 1.681 kPa (No. 1 heat exchanger), 1.732 kPa (No. 2 heat exchanger), 1.757 kPa (No. 3heat exchanger) and 1.807 kPa (No. 4 heat exchanger), respectively. Considering that the backpressure produced by the muffler usually varied from 4 kPa to 6 kPa, the increased exhaust flow resistance caused by the four chaos-shaped heat exchangers is acceptable and still needs further reducing since it may degrade the original fuel economy and dynamic performance of the prototype SUV. In all, according to the maximum power and backpressure of the AETEG when the SUV speed reaches its maximum value, the road test experimental results of the AETEG validate its promising potential for use in the ISG mild hybrid powertrain.

CONCLUSIONS

The hybrid powertrain application of the AETEG will be a further research focus even though the development of the AETEG is in the initial stage and its overall output power is not large enough, since it can improve the fuel economy of a vehicle by recycling the exhaust waste heat and decreasing the battery capacity to some extent. According to the established ISG mild hybrid powertrain system based on the AETEG, the parameter matching of all the components were analyzed with the basic vehicle dynamics theory, and all parameters were optimized based on the designed control strategy and different driving cycles. The simulation results based on the Urban Dynamometer Driving Schedule (UDDS), ECE_EUDC_LOW, and Highway Fuel Economy Test (HWFET) driving cycles validate that the dynamic performance is improved, the maximum speed of ISG mild hybrid powertrain approaches 142 km/h, the acceleration time from 0 km/h to 120 km/h is 18.9 s, and the fuel consumption is reduced by about 25%, which meets the designed performance requirements. The road test experimental results also indicate that the

maximum output power of the optimized AETEG is about 610 W, and the maximum backpressure is below 1.8 kPa when the highest vehicle speed is 125 km/h. The proposed parameter matching and optimization method in this paper is verified to be feasible and efficient, which can provide practical guidance for the future development of a hybrid powertrain system based on thermoelectricity.

ACKNOWLEDGMENTS

This paper has been supported by the National Natural Science Foundation of China (51977061, 51407063), and the Doctor Scientific Research Foundation of Hubei University of Technology (BSQD13064).

REFERENCES

1. P. Fernández-Yáñez, O. Armas, R. Kiwan, A.G. Stefanopoulou, and A.L. Boehman, *Appl. Energy* 229, 80 (2018).
2. F.J. Willars-Rodríguez, E.A. Chávez-Urbiola, P. Vorobiev, and Y.V. Vorobiev, *Int. J. Energy Res.* 41, 377 (2017).
3. M.E. Demir and I. Dincer, *Appl. Therm. Eng.* 120, 694 (2017).
4. W.K. Li, J.Y. Peng, W.L. Xiao, H.H. Wang, J.S. Zeng, J. Xie, and Q.B. Huang, *Appl. Therm. Eng.* 118, 742 (2017).
5. F.K. Meng, L.G. Chen, Y.L. Feng, and B. Xiong, *Energy* 135, 83 (2017).
6. T.Y. Kim, A.A. Negash, and G. Cho, *Energy Convers. Manag.* 124, 280 (2016).
7. D. Champier, *Energy Convers. Manag.* 140, 167 (2017).
8. W. Lee and J. Lee, *Energy Convers. Manage.* 171, 1302 (2018).
9. F. Soriano, M. Moreno-Eguilaz, J. Alvarez, and J. Riera, *Int. J. Automot. Technol.* 17, 873 (2016).
10. K. Oetringer, M. Kober, and M.K. Altstedde, in *Proceedings of the 9th International Conference on Ecological Vehicles and Renewable Energies* (2014).
11. S.K. Kim, B.C. Won, S.H. Rhi, S.H. Kim, J.H. Yoo, and J.C. Jang, *J. Electron. Mater.* 40, 778 (2011).
12. N. Kempf and Y.L. Zhang, *Energy Convers. Manag.* 121, 224 (2016).
13. X.L. Li, C.J. Xie, S.H. Quan, L. Huang, and W. Fang, *Appl. Energy* 231, 887 (2018).
14. A. Massaguer, E. Massaguer, M. Comamala, T. Pujol, J.R. González, M.D. Cardenas, D. Carbonell, and A.J. Bueno, *Appl. Energy* 222, 42 (2018).
15. X.L. Li, C.J. Xie, S.H. Quan, Y. Shi, and Z.B. Tang, *IEEE Access* 7, 72143 (2019).
16. S.W. Shen, J.Z. Zhang, X.J. Chen, Q.C. Zhong, and R. Thornton, *Veh. Syst. Dyn.* 48, 301 (2010).
17. D. Gagliardi and C. Wren, *Auto Technol.* 11, 30 (2011).
18. R. Yu, *Chem. Eng. Trans.* 46, 163 (2015).
19. Q.P. Chen, H.Y. Shu, B. Chen, J.H. Du, and S. Zhuang, *Int. J. Electr. Hybrid Veh.* 4, 248 (2012).
20. X.G. Wu, J.F. Chen, and J.Y. Du, in *Proceedings of the 28th International Electric Vehicle Symposium and Exhibition* (2015).
21. R. Quan, B.H. Tan, X.F. Tang, S.H. Quan, and L. Huang, *Zhongguo Jixie Gongcheng* 25, 705 (2014).
22. X. Liu, Y.D. Deng, K. Zhang, M. Xu, Y. Xu, and C.Q. Su, *Appl. Therm. Eng.* 71, 364 (2014).
23. R. Quan, X.F. Tang, S.H. Quan, and L. Huang, *J. Electron. Mater.* 42, 1469 (2013).
24. R. Quan, W. Zhou, G.Y. Yang, and S.H. Quan, *J. Electron. Mater.* 46, 2676 (2017).
25. P.C. Qiu, B.M. Ge, and D.Q. Bi, *Power Syst. Prot. Control* 39, 62 (2011).
26. X.L. Gou, H. Xiao, and S.W. Yang, *Appl. Energy* 87, 3131 (2010).
27. G. Fraisse, J. Ramousse, D. Sgorlon, and C. Goupil, *Energy Convers. Manag.* 65, 351 (2013).
28. G. Wu, C. Zhu, and C.C. Chan, *J. Asian Electr. Veh.* 8, 1357 (2010).
29. G. Wu, R. Lu, C. Zhu C, and C.C. Chan, in *Proceedings of the 2010 IEEE Vehicle Power and Propulsion Conference* (2010).
30. T. Markel, A. Brooker, T. Hendricks, V. Johnson, K. Kelly, B. Kramer, M. O'Keefe, S. Sprik, and K. Wipke, *J. Power Sources* 110, 255 (2002).